

Identifying weather patterns as sociated with increased volcanic ash risk within British Isles airspace

Article

Published Version

Creative Commons: Attribution 4.0 (CC-BY)

Open Access

Harrison, S. R., Pope, J. O., Neal, R. A., Garry, F. K., Kurashina, R. and Suri, D. (2022) Identifying weather patterns as sociated with increased volcanic ash risk within British Isles airspace. *Weather and Forecasting*, 37 (7). pp. 1157-1168. ISSN 0882-8156 doi: 10.1175/waf-d-22-0023.1 Available at <https://centaur.reading.ac.uk/105003/>

It is advisable to refer to the publisher's version if you intend to cite from the work. See [Guidance on citing](#).

To link to this article DOI: <http://dx.doi.org/10.1175/waf-d-22-0023.1>

Publisher: American Meteorological Society

All outputs in CentAUR are protected by Intellectual Property Rights law, including copyright law. Copyright and IPR is retained by the creators or other copyright holders. Terms and conditions for use of this material are defined in the [End User Agreement](#).

www.reading.ac.uk/centaur

CentAUR

Central Archive at the University of Reading

Reading's research outputs online

Identifying Weather Patterns Associated with Increased Volcanic Ash Risk within British Isles Airspace

SAMUEL R. HARRISON,^a JAMES O. POPE,^b ROBERT A. NEAL,^b FREYA K. GARRY,^b RYOSUKE KURASHINA,^c AND DAN SURI^b

^a *University of Reading, Reading, United Kingdom*

^b *Met Office, Exeter, United Kingdom*

^c *Imperial College London, London, United Kingdom*

(Manuscript received 16 February 2022, in final form 6 April 2022)

ABSTRACT: Icelandic volcanic emissions have been shown historically and more recently to have an impact on public health and aviation across northern and western Europe. The severity of these impacts is governed by the prevailing weather conditions and the nature of the eruption. This study focuses on the former utilizing an existing set of 30 weather patterns produced by the Met Office. Associated daily historical classifications are used to assess which weather patterns are most likely to result in flow from Iceland into four flight information regions (FIRs) covering the British Isles and North Atlantic, which may lead to disruption to aviation during Icelandic volcanic episodes. High-risk weather patterns vary between FIRs, with a total of 14 weather patterns impacting at least one FIR. These high-risk types predominantly have a northwesterly or westerly flow from Iceland into British Isles airspace. Analysis of the historical classifications reveals a typical duration for high-risk periods of 3–5 days, when transitions between high-risk types are considered. High-risk periods lasting over a week are also possible in all four FIRs. Additionally, impacts are more likely in winter months for most FIRs. Knowledge of high-risk weather patterns for aviation can be used within existing operational probabilistic weather pattern forecasting tools. Combined probabilities for high-risk weather patterns can be derived for the medium-range (1–2 weeks ahead) and used to provide a rapid assessment as to the likelihood of flow from Iceland. This weather pattern forecasting application is illustrated using archived forecast data for the 2010 Eyjafjallajökull eruption.

KEYWORDS: Europe; North Atlantic Ocean; Volcanoes; Air quality; Climate classification/regimes; Climate records; Ensembles; Forecasting; Health; Societal impacts

1. Introduction

On 8 June 1783 the Icelandic volcano Laki commenced a series of eruption events that continued until 7 February 1784 (Thordarson and Self 2003). In addition to producing 15.1 km³ of magma, the eruption generated 379 megatons of gaseous material over the duration of the eruption, including 122 megatons of sulfur dioxide (SO₂) and 235 megatons of water vapor (H₂O). These emissions resulted in the formation of ~200 megatons of hydrogen sulfate (H₂SO₄) which was injected into the upper troposphere with around 83% of total emissions released in the summer of 1783 (Thordarson and Self 2003). Owing to the atmospheric conditions over northern Europe at this time, an initial haze was reported in the far north of Scotland and the west coast of Norway on 10 June 1783. From mid-June a haze was reported across central Europe with reports by late June covering the area from Lisbon to Moscow (Thordarson and Self 2003). Through

the summer of 1783, a range of impacts were reported. These included decreased crop yields and damage to vegetation (Thordarson and Self 2003) and excess mortality in English parish (local area) records, around 10%–20% greater than the 51-yr average (Grattan et al. 2003; Schmidt et al. 2011). A modeling study replicating the 1783–84 Laki eruption and coincident meteorological conditions indicated that a similar Icelandic eruption in the present day would result in 142 000 additional cardiopulmonary deaths over Europe (Schmidt et al. 2011).

More recently, the explosive phase of the eruption of Eyjafjallajökull, which commenced on 14 April 2010 (Sigmundsson et al. 2010), resulted in a trachyandesite magma interacting with ice to augment an explosive eruption and the injection of a fine grained tephra to heights of between 6 and 9 km (Sigmundsson et al. 2010). The generation of this ash cloud resulted in the week-long closure of European airspace and the cancellation of 108 000 flights affecting 10.5 million passengers (Budd et al. 2011). The suspension of air travel had an economic impact of \$1.7 billion (U.S. dollars) on the aviation industry (Budd et al. 2011).

However, not all Icelandic volcanism impacts directly on the British Isles or continental Europe; for example the

 Denotes content that is immediately available upon publication as open access.

 Supplemental information related to this paper is available at the Journals Online website: <https://doi.org/10.1175/WAF-D-22-0023.s1>.

Corresponding author: Samuel R. Harrison, s.r.harrison@pgr.reading.ac.uk



This article is licensed under a [Creative Commons Attribution 4.0 license](http://creativecommons.org/licenses/by/4.0/) (<http://creativecommons.org/licenses/by/4.0/>).

DOI: 10.1175/WAF-D-22-0023.1

© 2022 American Meteorological Society. For information regarding reuse of this content and general copyright information, consult the [AMS Copyright Policy](https://www.ametsoc.org/PUBSReuseLicenses/) (www.ametsoc.org/PUBSReuseLicenses/).

19 March 2021 eruption of the Fagradalsfjall volcano, an effusive eruption (Cubuk-Sabuncu et al. 2021) has not generated any ash impacts, with gas impacts limited to the local area of Iceland. The 21 May 2011 eruption of the Grimsvotn volcano, believed to be the largest land-based Icelandic eruption since Katla in 1918 (Prata et al. 2017) generated a plume of ash, which peaked as high as 15–19 km, with levels around 8 km for much of the week after (Prata et al. 2017). Despite being a large ash generating volcanic eruption, similar to the 2010 Eyjafjallajökull eruption 13 months earlier, the impact of this eruption was limited, with just 900 flights cancelled (based on media reports) outside of Iceland, primarily impacting the northern United Kingdom and north and western Scandinavia.

A significant difference between the 2010 Eyjafjallajökull and 2011 Grimsvotn eruptions was the weather conditions during the week of the eruption. As discussed in Harvey et al. (2020), during the 2011 Grimsvotn eruption, there were significant low pressure systems between Scotland and Iceland. These conditions drove the flow from the volcano away from European airspace and also facilitated a higher rate of wet deposition of the ash, removing it from the atmosphere sooner (Harvey et al. 2020). These conditions were very different to those of the week commencing 14 April 2010 (Petersen 2010; Petersen et al. 2012; Stevenson et al. 2013), when a large high pressure system west of Ireland transported ash from the 2010 Eyjafjallajökull eruption from Iceland to western Europe.

The initial gas release phase of the 1783–84 Laki eruption initially bears some similarities to that of the 2011 Grimsvotn eruption. Analysis of contemporary weather station data (Kington 1988) suggested a region of low pressure between Iceland and Norway on 10 June 1783, which resulted in some initial minor impacts being observed in these localized regions (Thordarson and Self 2003). However, unlike the 2011 Grimsvotn eruption, the 1783–84 Laki event persisted through a change in the air flows. Here, low pressure developed over the British Isles by 17 June 1783 (Kington 1988), which generated a flow from Iceland into western Europe and eventually southern England. Through the summer of 1783, the conditions changed to a persistent high pressure system, leading to a prolonged summer haze, with still and calm conditions limiting deposition from the atmosphere (Thordarson and Self 2003).

Out of the four examples of Icelandic volcanism discussed above, two had wide-reaching impacts on the British Isles and Continental Europe and two had minimal or no impacts over the same area. There are two factors that influence whether there are impacts in sectors such as aviation or public health from Icelandic volcanism. The first relates to the type of eruption and the second to the airflow around Iceland. The former is by its very nature unpredictable. For example, the initial 2010 Eyjafjallajökull eruption in March 2010 was an effusive eruption on the flanks of the main vent, which occurred prior to the more explosive eruption that generated the ash cloud impacts in April 2010 (Sigmundsson et al. 2010). For the latter, historical analysis allows for the airflow around Iceland to be classified into sets of likely weather patterns that will drive ash and other deposits away from Iceland into the airspace of the British Isles and continental Europe—which is the focus of

this paper. It is then possible to use weather forecasting models to predict when these regions would be vulnerable to eruption conditions that would generate societal impacts.

In the context of this paper, a weather pattern can be defined as one of many large-scale circulation types over a predefined region (e.g., the British Isles and surrounding European area), which differs in its characteristics from other weather patterns over the same region and can vary on a daily basis (Neal et al. 2016). Weather regimes are another description for large-scale circulation types, but these tend to be fewer in number, larger in scale and persist for longer than weather patterns (e.g., Vautard 1990; Fereday et al. 2008; Ferranti et al. 2015). The occurrence of these circulation types can be predicted using numerical weather prediction (NWP) forecasting tools, whereby forecast fields are objectively assigned to the closest matching circulation-type definition. This works best if done using ensemble forecasting systems [such as those described by Buizza et al. (2007) and MacLachlan et al. (2015)] in order to capture increasing uncertainties as the forecast lead time increases, typically looking 1–2 weeks in advance (covering the medium-range outlook) and potentially 3–4 weeks in advance (covering the extended-range outlook). Here, circulation type probabilities can be based on the number of ensemble members objectively assigned to each type. For example, Ferranti and Corti (2011) present one of the first such forecasting examples, which presents forecast probabilities for a set of four predefined large-scale weather regimes for Europe, as described in detail by Ferranti et al. (2015). Neal et al. (2016) also present a circulation-type forecasting example, but this time using the set of 30 Met Office weather patterns for the British Isles and surrounding area, which are also used in this paper. This forecasting tool provides daily weather pattern probabilities and is used operationally at the Met Office for identifying the most likely weather pattern transitions within the medium- to extended-range period. These forecasts are also used for highlighting periods at risk of high impact weather, such as coastal flooding (Neal et al. 2018), fluvial flooding (Richardson et al. 2020), lightning risk (Wilkinson and Neal 2021), and extreme wave heights in the North Sea (Steele et al. 2017, 2018).

This paper will add to the set of weather pattern forecasting applications mentioned above by investigating the relationship between the set of 30 Met Office weather patterns (Neal et al. 2016) and flow from Iceland into U.K. airspace. To achieve this, the Met Office weather patterns will be combined with wind data from the ERA5 reanalysis (Hersbach et al. 2020) at a selection of levels through the troposphere to assess which weather patterns would generate a flow from Iceland that would impact on aviation in the flight information regions (FIRs) surrounding and covering the British Isles. We will then present an analysis of how long these patterns persist, which would lengthen the duration of the event and the socioeconomic impact. Finally we will demonstrate the application of this work through the use of a medium-range (one to two week) forecasting case study for the 2010 Eyjafjallajökull eruption. During the preparation of this paper (late 2021/early 2022), the Grimsvotn and Krysuvik volcanoes in Iceland both spent a period of time rated “Orange” on the

Icelandic Meteorological Office's Aviation Color Code system, highlighting that the risk of eruption is a regular concern.

2. Methods

a. The Met Office weather patterns and their forecasting application

This paper uses the existing set of 30 daily Met Office weather patterns described by Neal et al. (2016), which represent the full range of climatological circulation types affecting the United Kingdom and surrounding area. These patterns were created by applying a clustering algorithm to the European and North Atlantic Daily to Multi-Decadal Climate Variability (EMULATE; Ansell et al. 2006) dataset. EMULATE is a gridded daily historical MSLP anomaly dataset for a North Atlantic–European domain (30°W–20°E, 35°–70°N) at 5° horizontal resolution for the period 1850–2003. The clustering algorithm used by Neal et al. (2016) outputs a set of static weather pattern definitions [as mean sea level pressure (MSLP) anomaly fields] as well as a daily historical weather pattern classification dataset, which shows the observed weather pattern on each day between 1850 and 2003.

Here we use an updated daily historical weather pattern classification dataset for the period 1 January 1950–31 December 2020, which uses the ERA5 reanalysis (Hersbach et al. 2020). To produce this updated historical classification, 1200 UTC ERA5 MSLP fields were converted to anomalies (using a smoothed ERA5 daily climatology for the same period) before assigning them to the closest matching weather pattern definition (which are also defined according to their MSLP anomalies). The method used to assign reanalysis fields to weather patterns is based on the pairing with the smallest gridpoint average sum of squared differences and is explained in more detail by Neal et al. (2016). The daily historical weather pattern classifications provide a very useful dataset, as they enable us to generate weather pattern climatologies (e.g., for wind flow from Iceland), where daily reanalysis or observation fields exist. They also allow us to assess typical weather pattern persistence and transitions, which is useful in this study for understanding the typical duration and frequency of flow from Iceland events.

As there are a set number of climatological weather patterns, the MSLP reanalysis field for a given day is unlikely to perfectly match the assigned pattern. This is because each weather pattern represents a climatological ideal and there will be some variability within each type. As a result, the weather pattern classification contains an element of uncertainty between the known flow direction and the exact point of interaction. As such, it is not possible to state in this work that specific conditions will impact on a specific airport, but there is confidence to state when the pattern impacts on a regional area, such as an FIR.

As well as historical analysis, these weather patterns can be used within a forecasting context by assigning multiple forecast fields from an ensemble prediction system (EPS) to the closest matching weather pattern definition. The assignment method used here is the same as used for the reanalysis fields

described above. There are several EPSs available and here we use the 51-member 15-day ensemble run by the European Centre for Medium-Range Weather Forecasts (ECMWF) (Buizza et al. (2007)). Daily weather pattern forecast probabilities are derived by counting the number of ensemble members objectively assigned to each weather pattern and then dividing this number by the total number of ensemble members. Probabilities can then be aggregated for sets of high-risk “flow from Iceland” weather patterns, thereby providing a probability of flow from Iceland into U.K. airspace. Previous studies have objectively verified probabilistic weather pattern forecasts over Europe. Most relevant to this study, Neal et al. (2016) present forecast verification results related to the set of 30 weather patterns used in this study using the ECMWF ensemble. Ferranti et al. (2015) and Neal et al. (2016) show daily regime predictability out to at least 10 days, with predictability being better in winter than summer. Ferranti et al. (2015) also show similar levels of predictability over Europe using a set of four large-scale weather regimes. More recently, Büeler et al. (2021) show that useful skill could be extended out to three weeks when considering weekly probabilities.

b. ERA5 reanalysis winds

We evaluate the likely direction of the flow from Iceland for each weather pattern using the European Centre for Medium Range Weather Forecasting (ECMWF) ERA5 reanalysis (Hersbach et al. 2020). ERA5 is available with a horizontal resolution of 31 km and a daily temporal resolution used here for the period 1950–2020. Daily eastward (u) and northward (v) components of wind at 1200 UTC were downloaded from the Copernicus Climate Data Centre for four levels through the troposphere: 1000 hPa (the surface winds), 750 hPa (equivalent to ~2.5 km), 500 hPa (equivalent to ~5.5 km), and 300 hPa (equivalent to ~9 km) to provide a cross section of the troposphere. The cross section ensures we are able to assess variations between the weather patterns (determined using surface pressure) and winds that occur at different levels of the troposphere. This is particularly important as the injection of ash and gas occurs throughout the troposphere, therefore it is important to represent the winds associated with each weather pattern throughout the troposphere. For the weather pattern analysis the 1000- and 750-hPa heights refer to lower level flow with the 500- and 300-hPa heights referring to upper level flow.

c. Chained persistence of weather patterns

Prior analyses of the Met Office weather patterns (such as Pope et al. 2022) have focused on the frequency and persistence of individual patterns. If the weather pattern changed to another of the 30 weather patterns, then the persistence of the prior pattern was considered to have ended. However, there are a number of weather patterns that are very similar and they can be grouped together. For example, Neal et al. (2016) grouped the weather patterns into eight broad categories of circulation type such as patterns representative of the positive or negative phase of the North Atlantic Oscillation. As it is physically plausible for similar patterns to flip between

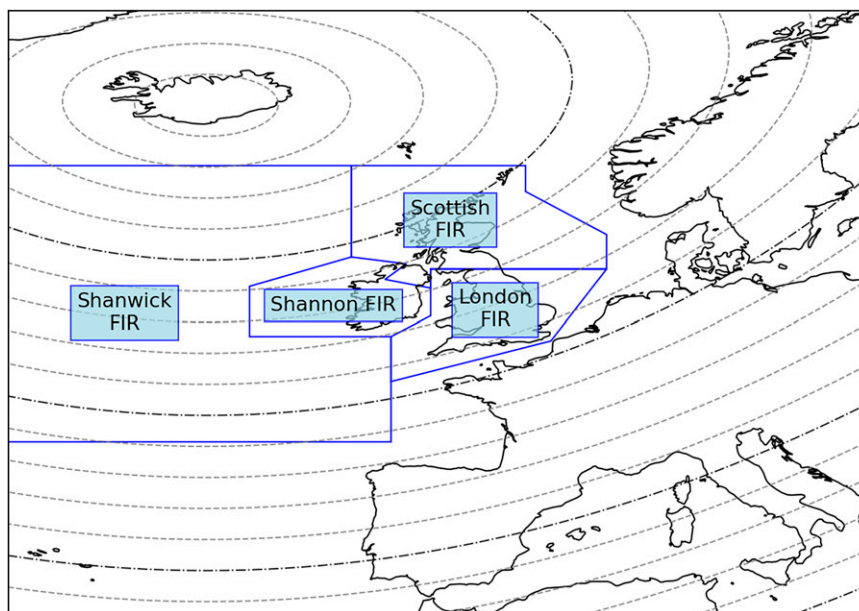


FIG. 1. A map displaying the approximate locations of the four FIRs (solid blue lines) with dashed lines displaying the radial distance from the center of Iceland at 200-km intervals, and dot-dash lines indicating a radial interval distance of 1000 km.

each other over a short time period, the persistence of a broad group is likely to be greater than of any individual pattern. Within the context of the flow from Iceland, the individual pattern is of less concern than the direction of flow. For example, northwesterly flow from Iceland will impact on some of the FIRs irrespective of whether that northwesterly flow is driven by weather pattern 13 or weather pattern 14, and it is feasible for these patterns to turn from one to the other and back again, while flow in a particular direction is maintained (see Fig. 1 in the online supplemental material).

Therefore to calculate the persistence of the events for each of the four FIRs, we assess the persistence of events by linking together all the weather patterns that are identified as bringing flow from Iceland into that FIR. For example, if over an 18-day period we observe the following weather patterns:

4-1-1-5-5-1-9-12-12-12-3-3-26-28-1-1-5-7.

If the weather patterns 1, 5, 6, 9, and 12 were in a grouping affecting an FIR (and the remaining 25 determined as not affecting the FIR), then individual persistence (treating each weather pattern individually as in Pope et al. 2022) would be 1.71 days (12 days of the patterns of interest in seven separate events). Alternatively, when we link the five patterns together for this set of days, the persistence value is 6 days (12 days of the patterns of interest in two separate events). Henceforth, we will refer to the persistence calculated based on linking together the patterns which affect an FIR as “chained persistence.”

d. Flight information regions

The airspace over the surface of Earth is divided into FIRs, with each FIR being managed by a controlling authority

which provides all the necessary air traffic services in that region. Airspace over the United Kingdom and eastern North Atlantic is divided into three FIRs (London, Scottish, and Shanwick), which surround the Irish controlled FIR of Shannon. The London FIR covers most of England and Wales up to a line that approximately runs from Blackpool to York. The Scottish FIR covers the rest of Great Britain and extends westward to encompass Northern Ireland to the boundary with the Shanwick FIR. Both the London and Scottish FIRs extend to cover the U.K. Exclusive Economic Zone (EEZ). The Shanwick FIR covers the eastern portion of the Atlantic Ocean. Approximately 80% of transatlantic flights go through the Shanwick FIR. The Shannon FIR covers the land area of the Republic of Ireland and extends to the boundaries of the Irish EEZ. Information on the FIRs was gathered from the U.K. National Air Traffic Services (NATS) website. The four FIRs are displayed in Fig. 1.

3. Results

a. Patterns affecting each FIR

In total, 14 weather patterns are associated with flow from Iceland into at least one of the FIRs for either the upper or lower levels (Fig. 2a). Predominantly these patterns result in northerly or northwesterly flow, driving emissions from Iceland toward the FIRs. Some patterns are associated with a low pressure centered over or just east of England, bringing flow south close to or over western Ireland and then round into southern England. The driving patterns are not all of a similar type, with anticyclonic, cyclonic, and unbiased patterns all contributing. While these 14 patterns affect all FIRs, it is important to distinguish between the different FIRs. For

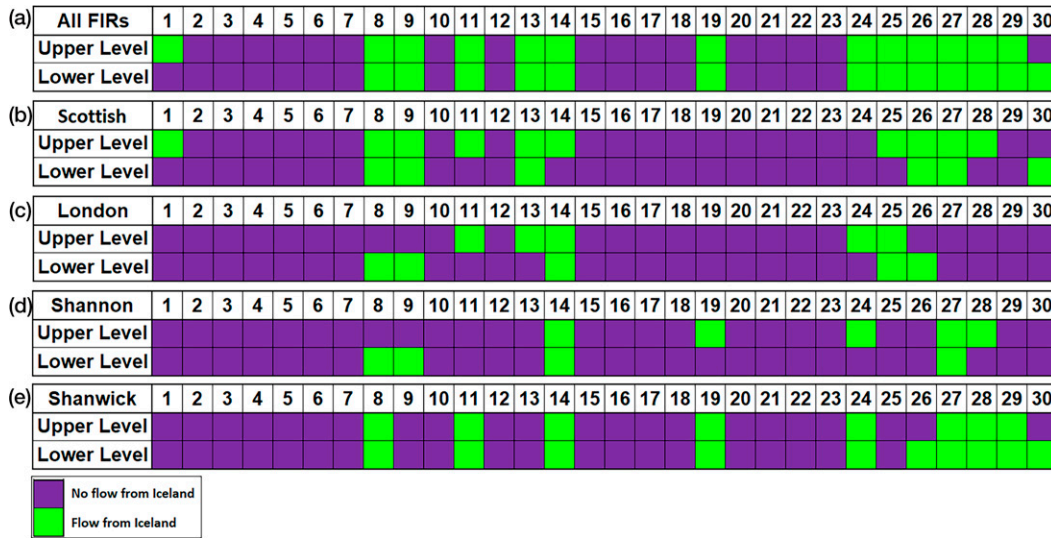


FIG. 2. The weather pattern (in green) that has been shown to derive flow from Iceland in either the upper or lower level for (a) All FIRs and then each individual FIR of interest, (b) Scottish, (c) London, (d) Shannon, and (e) Shanwick, using the boundaries as shown in Fig. 1.

example, an eruption affecting the Shanwick FIR at the upper levels would have a major impact on transatlantic flights, but would potentially have minimal impact on flights from the United Kingdom to continental Europe. Figures 2b–e indicate which of these 14 patterns impact on each of the four FIRs.

The streamflow images for all 30 weather patterns at the four troposphere slices (1000, 750, 500, and 300 hPa) can be found in the supplemental material, labeled as supplemental Fig. WPx, where x is the weather pattern number from 1 to 30.

1) SCOTLAND—PATTERNS: 1, 8, 9, 11, 13, 14, 25, 26, 27, 28, 30

The Scottish FIR is the most exposed FIR with respect to the number of patterns that result in flow from Iceland to an FIR. Patterns impacting on the Scottish FIR are split into several subgroups. Patterns 9, 13, 14, 25, 26, 28, and 30 are driven by northerly or northwesterly flow from Iceland. Predominantly these patterns represent an Atlantic high pressure west of Scotland and a region of low pressure centered over Scandinavia. Patterns 8, 11, and 30 are dominated by westerly or southwesterly flow, as a result of a region of low pressure centered over the United Kingdom. Pattern 27 features northeasterly flow (particularly in the midtroposphere), as a result of a high pressure ridge centered over Iceland. Pattern 1 features a similar set up to the first subgroup with a westerly flow driven by an Atlantic high pressure; however, the analysis of the wind patterns suggests that the impact on the Scottish FIR would be dependent on the explicit location of the region of high pressure. However, owing to its ability to impact on the FIR, it is included here in this analysis.

2) LONDON—PATTERNS: 8, 9, 11, 13, 14, 24, 25, 26

Patterns impacting upon the London FIR are split into two subgroups. Patterns 9, 13, 14, 25, and 26 represent northerly

or northwesterly flow direct to the London FIR having also impacted on Scottish FIR first. Patterns 8 and 11 represent westerly or southwesterly flow, whereby the flow from Iceland has initially headed south into the Atlantic before being wrapped around into Wales and Southern England again due to a low pressure system centered over the United Kingdom. These patterns also impact on the Scottish FIR; however, in this case they would impact on the London FIR first.

3) SHANNON—PATTERNS: 8, 9, 14, 19, 24, 27, 28

The Shannon FIR, nestling between the three U.K. FIRs is affected by a selection of the patterns influencing the Scottish and London FIRs. The one exception is pattern 19, which is a northerly flow from Iceland that impacts only on the Shannon and Shanwick FIRs, driven by a low pressure over the North Sea and high pressure in the Atlantic. The pattern is similar in type to pattern 14; however, the location of the pressure centers means it is less likely for this pattern to impact on Great Britain.

4) SHANWICK—PATTERNS: 8, 11, 14, 19, 24, 26, 27, 28, 29, 30

As with the three previous FIRs, the Shanwick FIR is affected predominantly by the groupings featuring northerly/northwesterly flow or westerly flow, such as patterns 8, 11, 14, 24, 26, 28, and 30 which also influence the London and Scottish FIRs. Shanwick is also impacted by pattern 27, as a result of the northeasterly flow in the midtroposphere. Like Shannon, the Shanwick FIR is impacted by the northerly flow from pattern 19; and unique to Shanwick are the impacts from pattern 29. Pattern 29, a strong low pressure, similar in structure to pattern 30, but with a center west of Ireland, could also produce some influences on the Shannon FIR;

however, these appear to be predominantly in the lower troposphere, and as a result aviation impacts could be minimal from this pattern.

5) MEAN FLOW SPEED

The streamflow figures (see supplemental Figs. WP1–WP30) provided a climatological flow speed in kilometers per day, with the four FIRs between 1000 and 2000 km from Iceland (Fig. 1). Given the unpredictability of volcanic eruptions, the speed of flow from Iceland will represent the preparation time before decisions on the airspace will be required to be made. There are a range of speeds associated with different weather patterns, for example, weather pattern 1 (supplemental Fig. WP1) has speeds of around 400–600 km day⁻¹ in the mid-upper troposphere, and as a result weather pattern 1 would take a couple of days to impact the Scottish FIR following an Icelandic eruption, whereas pattern 13 (supplemental Fig. WP13) has mid- to upper-tropospheric speeds of around 1700–2300 km day⁻¹, meaning that flow from Iceland could reach the Scottish and London FIRs within 12 h of the eruption commencing. The flow direction will also impact the arrival time into an FIR. Patterns 14 and 24 (supplemental Figs. WP14 and WP24) have comparable flow speeds in the mid- to upper troposphere, but different flow directions. Pattern 14 is a northwesterly flow regime and flow from Iceland proceeds directly to the Scottish and London FIRs, whereas pattern 24 flows south initially impacting the Shanwick FIR within a few hours of the eruption, but flow might take over 24 h to reach the London FIR as the flow direction is driven by the low pressure system over the United Kingdom. Both weather patterns would bring flow from Iceland that could impact on the airspace over the British Isles; however, the order and timing of airspace closure would be impacted by the weather pattern and the flow speed.

b. Chained persistence

While for the vast majority of patterns there would be impacts on the airspace around the British Isles within the first 24 h of the eruption, the impacts on aviation greatly increase as the duration of the event persists, both in the spatial extent as the ash can travel farther, but also in terms of the volume of passengers and freight affected. Therefore, while the frequency (or occurrence) of the weather pattern is necessary to assess the threat from the flow from Iceland, it is the persistence (or duration) of the event that would affect the magnitude of the impact. Previous analysis of the persistence of these weather patterns has focused on the persistence of individual weather patterns (Pope et al. 2022). Here we have used the concept of chained persistence to reflect that a number of the weather patterns are very similar and it is reasonable for their daily frequency to change from one to the other while maintaining flow from Iceland toward the British Isles.

For example, patterns 9, 13, and 14 all involve an Atlantic ridge of high pressure and a low pressure situated over Scandinavia. All three result in a northwesterly flow from Iceland into the Scottish and London FIRs (see supplemental Figs. WP9, WP13, and WP14), and as such it is reasonable to

include them together in an assessment of the event duration. In contrast, it is possible for patterns affecting an FIR to bring flow from different directions. For example, patterns 8 and 9 (supplemental Figs. WP8 and WP9) both affect the Scottish FIR; however, their different flow directions mean that a transition from pattern 9 to pattern 8 would not result in the impacts from the previous day being exacerbated in the next day. However, an analysis of the patterns from ERA5 (supplemental Fig. 1) demonstrates that on no occasion did pattern 8 transition into pattern 9 (or vice versa). This physical implausibility enables us to create the chained persistence based on all the weather patterns affecting each FIR.

Figure 3 highlights the difference between individual persistence and chained persistence for all the weather patterns that impact an FIR (Fig. 4 replicates this for the individual FIRs). For individual weather patterns, the persistence is dominated by 1- or 2-day events, with events rarely lasting 5 or more days. However, for the chained persistence, a one day event is as common as a 6-day event, with the majority of events lasting between 3 and 5 days. There are also a noticeable number of events that could last 8–10 days, similar to the events during the Eyjafjallajökull eruption in April 2010. Figure 4 highlights the same information for the different FIRs. As can be seen in Fig. 3, the chained persistence lengthens the duration of events in all the FIRs, with some differences between them. London and Scottish FIRs are dominated by the 2–6-day duration events, with very few events occurring for longer than a week in duration, with a similar distribution seen in Shannon (Fig. 4). While 2–6-day events are also the most common in Shanwick, they are less common than in the other FIRs (Fig. 4). However, unlike the other FIRs, Shanwick displays 2%–5% occurrence of events lasting 10–13 days, with noticeable durations of 16, 18, and 19 days (Fig. 4).

c. Seasonal variation in the frequency and persistence of these patterns

The 30 weather patterns used in this work are labeled from 1 to 30 based on their annual frequency (in the EMULATE dataset), with lower numbered patterns most common and higher numbered patterns least common annually (Neal et al. 2016). Within this, there is also a seasonal variation with different frequencies of weather patterns observed across the four meteorological seasons (Fig. 5). The winter and summer months are very different. In summer, the frequency of patterns 23–30 is less than 1%, but in winter, it is patterns 1–5 that rarely exceed 1% frequency. As such, it is plausible that one of these patterns would not occur on any day in that season in a given year. In spring and autumn, there is less variation in the frequency of each pattern, with the most patterns occurring between 2% and 5% of the time.

The seasonal variation in frequency of patterns impacts the potential occurrence of flow from Iceland toward the British Isles due to the tendency for higher numbered patterns to drive flow from Iceland. Figure 6 reveals the monthly frequency of the group of weather patterns which drive flow from Iceland toward the British Isles and its FIRs. The

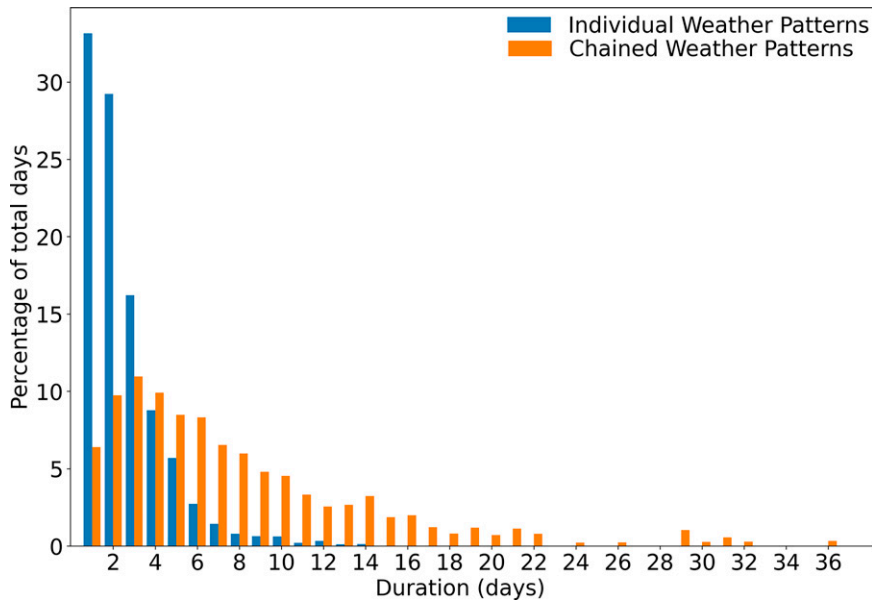


FIG. 3. Percentage of flow from Iceland event duration for the persistence of individual weather patterns (blue) and the chained persistence (orange), based on the ERA5 assigned weather patterns that influence any of the FIRs.

frequency of these patterns is around 35%–38% during October–April, but from May to September, the frequency is nearer 30%–33%. Also highlighted in Fig. 5 is the percentage of each individual pattern’s occurrence. Summer frequency is dominated by patterns 1, 8, and 9, which would have a larger impact on the Scottish FIR than the Shanwick FIR. When the monthly frequency of each pattern is assessed for the individual FIRs (Fig. 7), the impact of the different patterns becomes more evident. The London FIR displays minimal seasonality, with different patterns compensating for the seasonal changes in the frequency, for example winter frequency of pattern 25 decreases in the summer, when pattern 8 increases in frequency, as a result the seasonal frequency of the patterns for this FIR is between 24% and 26% in all months. The Scottish and Shannon FIRs display a slight seasonality, with winter frequency higher than in the summer and a transition through the spring and autumn months. Differences between winter and summer are around 4% in these two FIRs. The Shanwick FIR displays a considerable seasonality. As with Scottish and Shannon FIRs, this is dominated by winter patterns being more common than summer patterns in driving flow from Iceland; however, the difference between winter peak (~38% frequency) and summer peak (~18% frequency) is much greater at a change of around 20%. The transitions between seasons also show much sharper jumps, with the April–May (decrease) and September–October (increase) larger than the seasonality observed in the Scottish and Shannon FIRs.

d. Flow from Iceland forecast example for the 2010 Eyjafjallajökull eruption

The probabilistic weather pattern forecasting tool described in section 2a was not available at the time of the 2010

Eyjafjallajökull eruption. However, for the purposes of this case study we have extracted 51 ensemble forecast members from ECMWF’s archive from around this time and applied them to the weather pattern forecasting tool to see what sort of forecast signal would have been available. This provides us with an insight into how such a forecasting tool could be used in the present day to flag up forecast periods with the greatest likelihood of flow from Iceland. Probabilities of weather patterns occurring with a flow from Iceland component (high-risk types) are presented for all FIRs combined (Fig. 8) as well as having a breakdown of the likelihood of flow from Iceland into each of the four FIRs (supplemental Fig. 2).

As discussed in the introduction (section 1), the explosive and disruptive phase of the Eyjafjallajökull eruption began on 14 April 2010 and lasted for several days. However, the initial eruption began in March 2010 as an effusive (low impact) eruption on the flats of the main vent. Therefore, this volcano would have been undergoing significant monitoring as the Icelandic Meteorological Office does now with the aviation color code system (<https://en.vedur.is/earthquakes-and-volcanism/volcanic-eruptions/>). As such, an understanding of future flow conditions would have been helpful for contingency planning, particularly where forecasts extend into the medium range. For this reason, Fig. 8 presents the probability of weather patterns occurring which would bring flow from Iceland into U.K. airspace using an ECMWF forecast run initialized over a week before the main explosive eruption began.

In Fig. 8, the first five days of the forecast (which was initialized at 0000 UTC 6 April 2010) show a 0% probability of flow from Iceland. The probabilities then increase to around 70% over the following two days (up to 12 April 2010) and then persist at this level right out to the end of the 15-day forecast

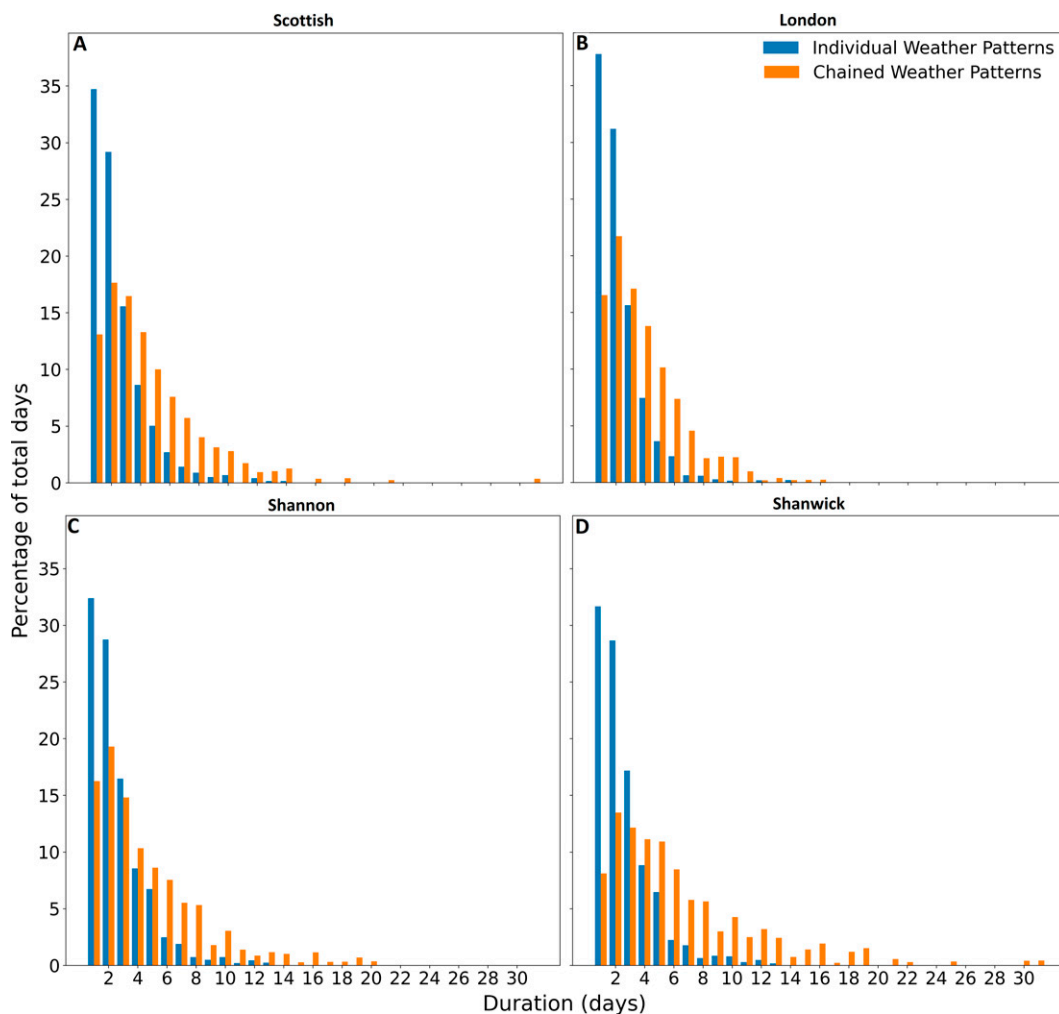


FIG. 4. As in Fig. 3, but for the four individual FIRs (a) Scotland, (b) London, (c) Shannon, and (d) Shanwick, based on the ERA5 assigned weather patterns that influence the respective FIRs.

period. Forecast probabilities are significantly above the 42% climatological occurrence for the time of year (as shown by the dashed horizontal lines) suggesting that flow from Iceland is much more likely than normal. In addition, the high forecast probabilities persist for an unusually long time. These high probabilities last for 9 days (between 12 April 2010 and 20 April 2010) covering the end of the forecast period. This compares to an average persistence of 3–5 days (Results; section 3b). Therefore, the combination of forecast probabilities higher than climatology for the time of year and the unusually long persistence of these high probabilities help flag the period from 12 April 2010 onward as being at a high risk of disruption should an explosive phase of the volcano emerge. Forecast confidence could be further improved by considering output from additional ensemble models (e.g., as provided by the Met Office Global Seasonal Forecasting System (GloSea; MacLachlan et al. 2015). In addition, an assessment of forecast consistency over consecutive runs could aid with forecast confidence.

Following an assessment of forecast probabilities for all FIRs combined, we look at the probabilities for each individual FIR to see if any are at a higher risk of disruption than others. The list of high-risk weather patterns varies slightly between each FIR (Fig. 2), therefore it is likely the probabilities will also vary depending on the weather patterns being forecast. For example, supplemental Fig. 2 shows the probabilities of flow from Iceland for each FIR separately using the same forecast initialization date as in Fig. 8. Here, the Scottish FIR has the highest probabilities, particularly for upper level flow. This is followed by Shannon and Shanwick FIRs which have slightly lower probabilities than the Scottish FIR, but still with probabilities considerably higher than climatology. Finally, probabilities for the London FIR are the lowest of all FIRs and hover only slightly higher than climatology from 12 April 2010 onward.

These forecasts are intended as a decision aid for meteorologists, providing a rapid assessment of the risk of volcanic ash originating over Iceland being transported into U.K. airspace.

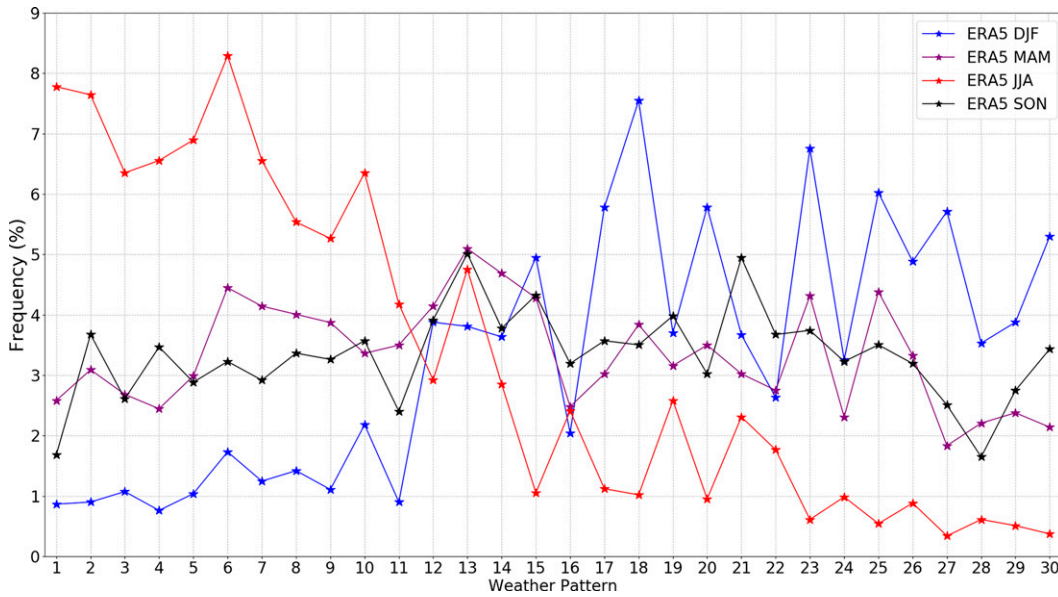


FIG. 5. Seasonal frequency of each ERA5 assigned weather pattern. Each color represents a different season, winter [DJF (blue)], spring [MAM (purple)], summer [JJA (red)], and autumn [SON (black)].

These forecasts are designed for use from days five or six onward (as highlighted by the hatching in the forecast example; Fig. 8) due to the large spatial scales involved. They will only provide the likelihood of wind flow from Iceland, with dispersion simulations still required from models such as the Met Office Numerical Atmospheric Modeling Environment

(NAME; Jones et al. 2007) to accurately assess the concentrations and specific locations of volcanic ash. As such, the weather pattern forecasts are not suitable for the issuance of aviation ash warnings, but instead could be used to provide written forecast guidance for contingency planning purposes and for organizational based internal preparedness.

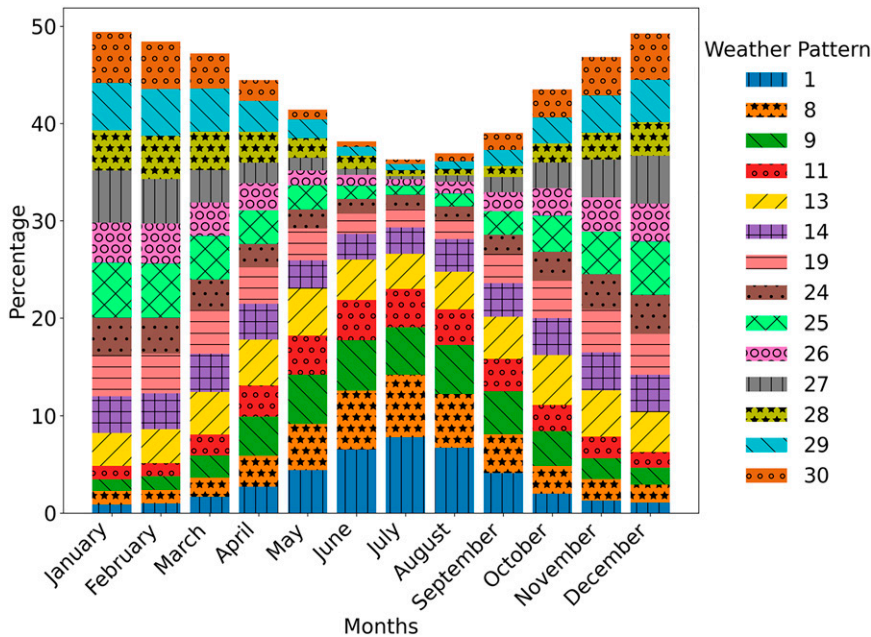


FIG. 6. Monthly frequency of each weather pattern to indicate the percentage of days when the patterns occur during the month, based on the ERA5 assigned weather patterns that influence any of the FIRs.

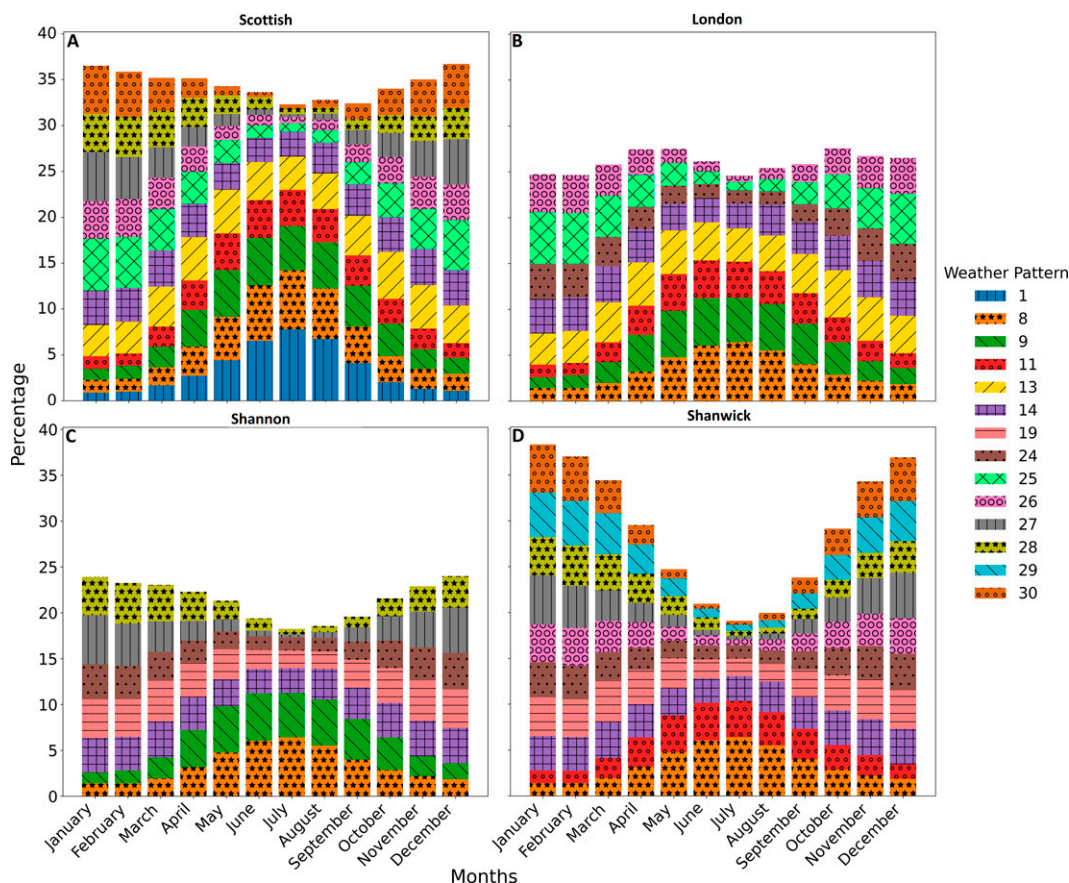


FIG. 7. As in Fig. 6, but for the four individual FIRs, (a) Scottish, (b) London, (c) Shannon, and (d) Shanwick, based on the ERA5 assigned weather patterns that influence the respective FIRs.

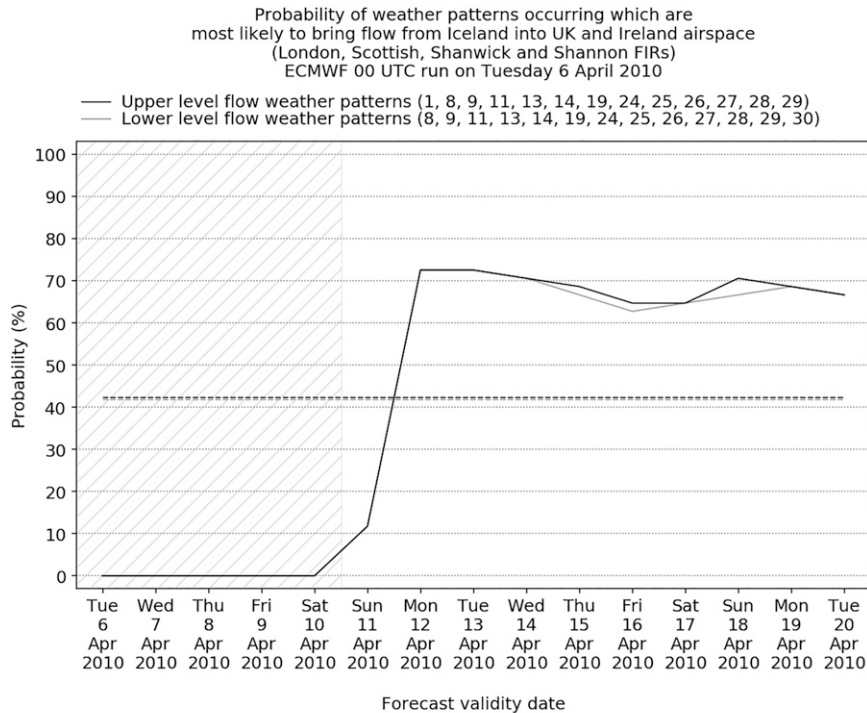
4. Conclusions

Since the 2010 Eyjafjallajökull eruption, the awareness of the impact of Icelandic volcanism on the British Isles and continental Europe has significantly increased. Here we present how a set of 30 weather patterns, currently used in operational numerical weather prediction tools to produce probabilistic medium-range forecasts, can be utilized to determine periods of high risk of flow from Iceland into specific regions, focusing on the four flight information regions covering the British Isles and eastern North Atlantic. By producing the streamflow from Iceland for each of the 30 weather patterns, we determined that 14 weather patterns were associated with flow from Iceland into at least one FIR. The patterns were predominantly in two groupings, either northerly and northwesterly flow or westerly and southwesterly flow into the FIRs. A second consideration in addition to the flow direction was the climatological flow speed, with different patterns resulting in varying times between the eruption of the ash and its arrival into an FIR (with the ability to impact on aviation).

The persistence of the flow into each FIR was also considered, through the assessment of “chained persistence,” focusing on the duration of patterns maintaining a consistent flow

from Iceland into an FIR, over the persistence of individual patterns. The four FIRs all displayed persistence of 3–5 days, with events occurring longer than a week particularly possible in the Shanwick FIR. Owing to the seasonality of the different weather patterns (lower numbered patterns more common in the summer and higher numbered patterns more common in the winter), there was also a seasonal variation in the occurrence of flow from Iceland affecting the FIRs, with a bias toward a higher risk in the winter months compared to the summer. A case study, using forecast fields from 6 April 2010, demonstrated how these weather patterns could be used as a medium-range (day five onward) decision aid for meteorologists assessing the potential for flow from Iceland to impact on British Isles airspace, with a view to providing contingency planning purposes and organization preparedness. It would still be necessary for dispersion models to accurately assess ash concentrations and provide short range aviation ash warnings.

Finally, studies of previous events (such as the 1783–84 Laki eruption) have highlighted the risk to public health from Icelandic volcanism (Thordarson and Self 2003; Schmidt et al. 2011). While the example in section 3d focused on an ash cloud event, it is plausible that the same patterns could be



Please note:

- Hatching indicates forecast lead times when higher resolution forecasts should be used.
- Dashed horizontal lines indicate climatological occurrence of weather pattern groups.

FIG. 8. The forecast probability of weather patterns occurring which are most likely to bring flow from Iceland into U.K. airspace based on the 0000 UTC ECMWF ensemble run initialized on 5 Apr 2010. Horizontal dashed lines show the climatological occurrence of the high-risk weather pattern groups relative to the time of year, and solid lines show the forecast probabilities.

used as a forewarning of a potential public health event. A future development of this work would be to understand the relationship between these patterns and the transport and deposition of volcanic gases that can impact on public health.

Acknowledgments. SRH and RK are funded by U.K. Engineering and Physical Sciences Research Council (EPSRC) Centre for Doctoral Training in Mathematics of Planet Earth. JOP was supported by the Met Office Climate Service for Food, Farming and Natural Environment, funded by the Department for Environment, Food and Rural Affairs (Defra) Climate Service. RN was funded by Met Office science. FG acknowledges the Strategic Priority Fund for U.K. Climate Resilience. The U.K. Climate Resilience Programme is supported by the UKRI Strategic Priorities Fund. The program is co-delivered by the Met Office and NERC on behalf of UKRI partners AHRC, EPSRC, and ESRC.

Data availability statement. The historical daily weather pattern classifications (up to 2020) are available on PANGAEA (Neal 2022). The streamflow plots for all 30 weather patterns are also included in the supplemental information as supplemental Fig. WP x where x is the number of the weather pattern.

These figures follow the supplemental figures referred to in the paper (supplemental Figs. 1 and 2).

REFERENCES

Ansell, T. J., and Coauthors, 2006: Daily mean sea level pressure reconstructions for the European–North Atlantic region for the period 1850–2003. *J. Climate*, **19**, 2717–2742, <https://doi.org/10.1175/JCLI3775.1>.

Budd, L., S. Griggs, D. Howarth, and S. Ison, 2011: A fiasco of volcanic proportions? Eyjafjallajökull and the closure of European airspace. *Mobilities*, **6**, 31–40, <https://doi.org/10.1080/17450101.2011.532650>.

Buizza, R., J. Bidlot, N. Wedi, M. Fuentes, M. Hamrud, G. Holt, and F. Vitart, 2007: The new ECMWF VAREPS (variable resolution ensemble prediction system). *Quart. J. Roy. Meteor. Soc.*, **133**, 681–695, <https://doi.org/10.1002/qj.75>.

Büeler, D., L. Ferranti, L. Magnusson, J. F. Quinting, and C. M. Grams, 2021: Year-round sub-seasonal forecast skill for Atlantic–European weather regimes. *Quart. J. Roy. Meteor. Soc.*, **147**, 4283–4309, <https://doi.org/10.1002/qj.4178>.

Cubuk-Sabuncu, Y., K. Jónsdóttir, C. Caudron, T. Lecocq, M. M. Parks, H. Geirsson, and A. Mordret, 2021: Temporal seismic velocity changes during the 2020 rapid inflation at Mt.

- Porbjörn-Svartsengi, Iceland, using seismic ambient noise. *Geophys. Res. Lett.*, **48**, e2020GL092265, <https://doi.org/10.1029/2020GL092265>.
- Fereday, D. R., J. R. Knight, A. A. Scaife, C. K. Folland, and A. Philipp, 2008: Cluster analysis of North Atlantic–European circulation types and links with tropical Pacific sea surface temperatures. *J. Climate*, **21**, 3687–3703, <https://doi.org/10.1175/2007JCLI1875.1>.
- Ferranti, L., and S. Corti, 2011: New clustering products. *ECMWF Newsletter*, No. 127, ECMWF, Reading, United Kingdom, 6–11, <https://doi.org/10.21957/lr3bcise>.
- , —, and M. Janousek, 2015: Flow-dependent verification of the ECMWF ensemble over the Euro-Atlantic sector. *Quart. J. Roy. Meteor. Soc.*, **141**, 916–924, <https://doi.org/10.1002/qj.2411>.
- Grattan, J. P., M. Durand, and S. Taylor, 2003: Illness and elevated human mortality coincident with volcanic eruptions. *Volcanic Degassing*, C. Oppenheimer, D. M. Pyle, and J. Barclay, Eds., Geological Society Special Publications, Vol. 213, Geological Society, 401–414.
- Harvey, N. J., H. F. Dacre, H. N. Webster, I. A. Taylor, S. Khanal, R. G. Grainger, and M. C. Cooke, 2020: The impact of ensemble meteorology on inverse modeling estimates of volcano emissions and ash dispersion forecasts: Grímsvötn 2011. *Atmosphere*, **11**, 1022, <https://doi.org/10.3390/atmos11101022>.
- Hersbach, H., and Coauthors, 2020: The ERA5 global reanalysis. *Quart. J. Roy. Meteor. Soc.*, **146**, 1999–2049, <https://doi.org/10.1002/qj.3803>.
- Jones, A. R., D. J. Thomson, M. Hort, and B. Devenish, 2007: The U.K. Met Office’s next-generation atmospheric dispersion model, NAME III. *Air Pollution Modeling and Its Application XVII (Proceedings of the 27th NATO/CCMS International Technical Meeting on Air Pollution Modelling and its Application)*, C. Borrego and A. L. Norman, Eds., Springer, 580–589.
- Kington, J. A., 1988: *The Weather of the 1780s over Europe*. Cambridge University Press, 166 pp.
- MacLachlan, C., and Coauthors, 2015: Global seasonal forecast system version 5 (GloSea5): A high-resolution seasonal forecast system. *Quart. J. Roy. Meteor. Soc.*, **141**, 1072–1084, <https://doi.org/10.1002/qj.2396>.
- Neal, R., 2022: Daily historical weather pattern classifications for the UK and surrounding European area (1950 to 2020). PANGAEA, accessed 4 April 2022, <https://doi.org/10.1594/PANGAEA.942896>.
- , D. Fereday, R. Crocker, and R. Comer, 2016: A flexible approach to defining weather patterns and their application in weather forecasting over Europe. *Meteor. Appl.*, **23**, 389–400, <https://doi.org/10.1002/met.1563>.
- , R. Dankers, A. Saulter, A. Lane, J. Millard, G. Robbins, and D. Price, 2018: Use of probabilistic medium- to long-range weather-pattern forecasts for identifying periods with an increased likelihood of coastal flooding around the UK. *Meteor. Appl.*, **25**, 534–547, <https://doi.org/10.1002/met.1719>.
- Petersen, G. N., 2010: A short meteorological overview of the Eyjafjallajökull eruption 14 April–23 May 2010. *Weather*, **65**, 203–207, <https://doi.org/10.1002/wea.634>.
- , H. Björnsson, and P. Arason, 2012: The impact of the atmosphere on the Eyjafjallajökull 2010 eruption plume. *J. Geophys. Res.*, **117**, D00U07, <https://doi.org/10.1029/2011JD016762>.
- Pope, J. O., K. Brown, F. Fung, H. M. Hanlon, R. Neal, E. J. Palin, and A. Reid, 2022: Investigation of future climate change over the British Isles using weather patterns. *Climate Dyn.*, **58**, 2405–2419, <https://doi.org/10.1007/s00382-021-06031-0>.
- Prata, F., M. Woodhouse, H. E. Huppert, A. Prata, T. Thordarson, and S. Carn, 2017: Atmospheric processes affecting the separation of volcanic ash and SO₂ in volcanic eruptions: Inferences from the May 2011 Grímsvötn eruption. *Atmos. Chem. Phys.*, **17**, 10709–10732, <https://doi.org/10.5194/acp-17-10709-2017>.
- Richardson, D., R. Neal, R. Dankers, K. Mylne, R. Cowling, H. Clements, and J. Millard, 2020: Linking weather patterns to regional extreme precipitation for highlighting potential flood events in medium- to long-range forecasts. *Meteor. Appl.*, **27**, e1931, <https://doi.org/10.1002/met.1931>.
- Schmidt, A., B. Ostro, K. S. Carslaw, M. Wilson, T. Thordarson, G. W. Mann, and A. J. Simmons, 2011: Excess mortality in Europe following a future Laki-style Icelandic eruption. *Proc. Natl. Acad. Sci. USA*, **108**, 15710–15715, <https://doi.org/10.1073/pnas.1108569108>.
- Sigmundsson, F., and Coauthors, 2010: Intrusion triggering of the 2010 Eyjafjallajökull explosive eruption. *Nature*, **468**, 426–430, <https://doi.org/10.1038/nature09558>.
- Steele, E., R. Neal, C. Bunney, B. Evans, N. Fournier, P. Gill, K. Mylne, and A. Saulter, 2017: Making the most of probabilistic marine forecasts on timescales of days, weeks and months ahead. *Offshore Technology Conf. (OTC)*, OTC-27708-MS, Houston, TX, <https://doi.org/10.4043/27708-MS>.
- , and Coauthors, 2018: Using weather pattern typology to identify calm weather windows for local marine operations. *Offshore Technology Conf. (OTC)*, OTC-28784-MS, Houston, TX, <https://doi.org/10.4043/28784-MS>.
- Stevenson, J. A., and Coauthors, 2013: UK monitoring and deposition of tephra from the May 2011 eruption of Grímsvötn, Iceland. *J. Appl. Volcanol.*, **2**, 3, <https://doi.org/10.1186/2191-5040-2-3>.
- Thordarson, T., and S. Self, 2003: Atmospheric and environmental effects of the 1783–1784 Laki Eruption: A review and reassessment. *J. Geophys. Res.*, **108**, 4011, <https://doi.org/10.1029/2001JD002042>.
- Vautard, R., 1990: Multiple weather regimes over the North Atlantic: Analysis of precursors and successors. *Mon. Wea. Rev.*, **118**, 2056–2081, [https://doi.org/10.1175/1520-0493\(1990\)118<2056:MWROTN>2.0.CO;2](https://doi.org/10.1175/1520-0493(1990)118<2056:MWROTN>2.0.CO;2).
- Wilkinson, J., and R. Neal, 2021: Exploring relationships between weather patterns and observed lightning activity for Britain and Ireland. *Quart. J. Roy. Meteor. Soc.*, **147**, 2772–2795, <https://doi.org/10.1002/qj.4099>.